Burgess, P.M., Zhang, J., and Steel, R., 2022, Narrow is normal: Exploring the extent and significance of flooded marine shelves in icehouse, transitional, and greenhouse climate settings: Geology, https://doi.org/10.1130/G49468.1

SUPPLEMENTAL MATERIAL

Supplemental data and worked example interpreting marine to non-marine topset strata to estimate marine topset width and associated uncertainty

Determination of marine topset shelf width from seismic, well-log and outcrop data

We have measured the maximum width of the marine shelf portion of clinoform topsets from 10 depositional systems spanning icehouse, transitional and greenhouse climate settings (Table S1). In each case the clinoform strata show repeated regressive-transgressive episodes that can be identified by several means in the outcrop, well-log and seismic data we used in this study. In each transgressive-regressive cycle, we define marine shelf width as the distance from the most landward location where the marginal marine strata pass landwards to nonmarine strata, marking the point of maximum landward shoreline transgression, to the most distal position of the clinoform break-of-slope, marking the most distal position of the shoreline in the previous regressive phase strata.

Measurement requires identification of both of these points for each cycle. This is quite straight forward from the seismic data we use because the lateral extent of thin-but-seismically slow fine grained sediment deposited as shelf drape during shoreline transgression is well imaged (see main text, figure 1B). The interpretation process is slightly more complicated in outcrop however, and particularly in well-log data, but the essential observation is the point basal fine-grained marine strata in upward-coarsening units pinch out, and where more sand-prone topset strata change to more mud-prone slope strata. In both outcrop and well log data, sand versus mud content of the strata is an initial guide, with more proximal fluvial strata being more sand-prone, and more distal marine slope being the most mud prone (Steel et al 2002; Zhang et al 2017). In outcrop, multiple lines of observation evidence, from basic lithology to sedimentary structures and ichnofabrics are used to reconstruction depositional process and environment, thus identifying the position of the shoreline and shelf edge through time. Diagnostic information is less abundant in the gamma ray well-log data, but the log responses do indicate sand proportion and style of deposition, for example thick-versus thin-bedded, blocky versus coarsening-or-fining-upwards. These log responses are used to interpret depositional settings from coastal plain topset, to deep-water toeset strata, to correlate the well-log data to define interpreted isochronous chronostratigraphic surfaces.

From this interpretation process, for each regressive-transgressive cycle, we can locate the position of the most landward point of shoreline transgression (Figure 1, blue triangles), and the position of the most distal position on the clinoform break-of-slope (Figure 1, red triangles) can also be identified. Distance between red and blue triangle pairs along the same chronostratigraphic surface defines marine topset shelf width. Detailed results from these measurements are available in the associated Excel worksheets (Table S2).

Estimates of measurement uncertainty

There are several sources of uncertainty in this interpretation process, all of which could impact on the accuracy of the final estimated marine topset width. Data point spacing in these data sets is generally good, so the maximum uncertainty in identifying the regressive-transgressive end points is not more than a few kilometers in the outcrop and well log data, and probably less in the seismic data, depending on the distance of marine mud strata lateral pinchout up-dip once below seismic resolution. More difficult to estimate is the uncertainty in the outcrop and well-log interpretation of depositional environment. We estimate that given the changes in sand thickness and more detailed log responses, our interpretation of the position of the pinchout of marine strata up-dip is unlikely to wrong by more than one or two well log or outcrop locations, suggesting an error on the up-dip and down-dip termination positions in the order of 5km, or less if the data point spacing is closer.

The other key estimate in the analysis is the estimate of total topset length, made in order to normalize the marine topset lengths to the total length of the depositional system from up-dip pinchout of all strata to the shelf-slope-break position. In this case we use available paleogeographic maps and reconstructions to estimate the total length. In terms of total extent of strata up-dip, these are probably reasonably accurate, but what they do not account for so well is the possibility of subsequent erosion, such that what appears to be up-dip pinchout is actually up-dip truncation. The consequence of this is that some or perhaps even many of the estimates of total length are underestimates, leading to an overestimate of the proportion of the total depositional length that was marine topset.

Table S1. Details of clinoform topset systems analysed in this study.

Location/System name	Reference	Age	Climate setting	Data types	Number of measured topsets	Minimum width (km)	Mean width (km)	Maximum width (km)	Mean normalized width	Mean kilometers width all (km)	Mean normalized width all (km)
Washakie Basin margin, south central Wyoming	Carvajal (2007)	Maastrichtian	Greenhouse	Well data	16	18.00	42.26	57.50	0.49	18.77	0.33
Lower Wilcox, Gulf of Mexico, south Texas	Zhang et al. (2016); Zhang et al (2017)	Paleocene		well data	10	16.88	24.56	29.89	0.11		
Central Basin margin, Spitsbergen	Steel and Olsen (2002)	Eocene		Outcrops	12	3.50	4.97	10.00	0.16		
El Marcet, Catalan Coastal Range	Steel et al. (2000)	Eocene		Outcrops	7	2.00	3.29	5.00	0.55		
Northern Gulf of Mexico margin	Pers. Com., Olariu (2021)	Miocene	Transitional	Well data	8	70.00	80.11	100.00	0.58	72.13	0.43
Zambesi margin, Mozambique Channel, E. Africa	Jean-Pierre et al. (2018)	Late Miocene to Pleistocene		Seismic data	7	42.60	57.55	68.50	0.32		
Orinoco margin, Offshore Trinidad	Dixon (2005)	Pliocene		Seismic, well logs, outcrops	9	60.00	78.71	105.00	0.39		
Gulf of Mexico margin	Bhattacharya et al., 2019	Late Pleistocene	Icehouse	Seismic	4	60.00	82.50	100.00	0.75	93.67	0.72
Rhône margin, France	Lobo & Ridente (2014)	Late Pleistocene		Seismic	3	100.00	127.50	150.00	0.61		
Bengal margin, Bangladesh	Hübscher & Spieß (2005)	Late Pleistocene		Seismic	4	60.00	71.00	85.00	0.79		

References for data in Table S1

Bhattacharya, J., Miall, A.D., Ferron, C., Gabriel, J. Randazzo, N., Kynaston, D., Jicha, B. and Singer, B.S, 2019. Time stratigraphy in point-sourced deltas: applications to sediment budgets shelf construction and paleo-storm records. Earth Science Reviews 199, 102985

Carvajal, 2007, Sediment volume partitioning, topset processes and clinoform architecture, understanding the role of sediment supply, sea level and delta types in shelf-margin building and deepwater sand bypass; the Lance-Fox Hills Lewis system. PhD dissertation, UT Austin.

Dixon, R., 2005. Field Trip to Examine Outcrops of the Mayaro Fm, Mayaro Beach, SE Trinidad. The Geological Society of Trinidad & Tobago.

Hübscher, C., and Spieß, V., 2005. Forced regression systems tracts on the Bengal Shelf. Marine Geology, 219 (4), 207–218.

Jean-Pierre, P., Robin, Cé., Guillocheau, Franç., Popescu, S., Suc, J.-P., Dall'Asta, M., Melinte-Dobrinescu, M.C., Bubik, M., Dupont, Gé., Gaillot, Jé., 2018. The Zambezi delta (Mozambique channel, East Africa): High resolution dating combining bio-orbital and seismic stratigraphy to determine climate (palaeoprecipitation) and tectonic controls on a passive margin, Marine and Petroleum Geology. doi: 10.1016/j.marpetgeo.2018.07.017.

Lobo, F. J., and Ridente, D., 2014. Stratigraphic architecture and spatio-temporal variability of high-frequency (Milankovitch) depositional cycles on modern continental margins: An overview. Marine Geology, 352, 215–249.

Steel, R.J. and Olsen, T., 2002. Clinoforms, clinoform trajectories and deep-water sands. Proceedings of 22nd Annual Gulf Coast Section SEPM Foundation Bob Perkings Research Conference, p. 367-380 .

Steel, R.J., Rasmussen H., Eide, S., Neumann, B. and Siggerud, E., 2000. Anatomy of high sediment-supply tracts in the Vilomara composite sequence, St. Llorenc del Munt, Catalan Range/Ebro Basin, NE Spain.

Zhang, J., Steel, R.J. and Ambrose, W., 2016. Greenhouse shoreline migration: Wilcox deltas. AAPG bulletin, 100, p.1803-1831.

Zhang, J., Steel, R.J. and Ambrose, W., 2017. Paleocene Wilcox cross-shelf channel-belt history and shelf-margin growth: Key to Gulf of Mexico sediment delivery. Sedimentary Geology, 362, p.53-65.

Figure Caption

Figure S1. Well-log correlation panel from the Washakie and Great Divide Basin in South Wyoming, landward-to-left, basinward-to-right, for clinothem strata in the Laramide Washakie/Great Divide Basin in southern Wyoming. Horizontal scale is ~3 km between each well. Red triangle symbols mark peak regression to shelf-slope break for each clinothem, blue triangle symbols mark the minimum landward distances reached by the marine transgressive half-cycle deposits. See text for discussion.

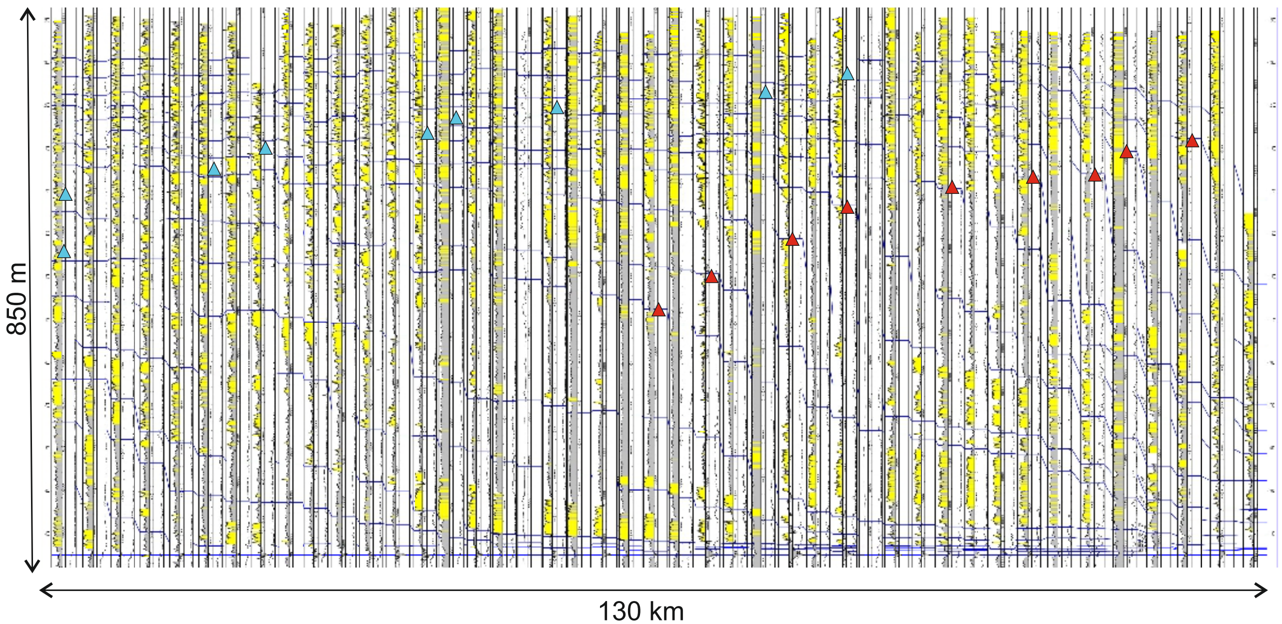

Fig. S1